In Situ Transmission Electron Microscopy Observation of Electrochemical Sodiation of Individual Co_9S_8-Filled Carbon Nanotubes

Qingmei Su,[†,‡] Gaohui Du,[†,*] Jun Zhang,[†] Yijun Zhong,[†] Bingshe Xu,[‡] Yuehai Yang,[§] Suman Neupane,[§] and Wenzhi Li[§,*]

[†]Institute of Physical Chemistry, Zhejiang Normal University, Jinhua 321004, China, [‡]College of Materials Science and Engineering, Taiyuan University of Technology, Taiyuan 030024, Shanxi, China, and [§]Department of Physics, Florida International University, Miami, Florida 33199, United States

ABSTRACT The comprehension of fundamental electrochemical behavior and sodiation mechanism is critical for the design of high-performance electrode materials for sodium-ion (Na-ion) batteries. In this paper, the electrochemical sodiation process and microstructure evolution of individual Co_9S_8-filled carbon nanotubes (CNTs) have been directly visualized and studied using *in situ* transmission electron microscopy. Upon the first sodiation, a reaction front propagates progressively along the filling nanowire, causing the filled CNT to inflate. The filled CNTs behave differently depending on their structures and the magnitude of the sodiation voltage. For a Co_9S_8-filled CNT with an open end, the sodiated Co_9S_8 filler shows a substantial axial elongation of 120.8% and a small radial swelling due to the extrusion of CNT walls. In contrast, the closed CNT shows a major radial expansion of 40.6% and a small axial elongation because of the mechanical confinement of the carbon shells. After sodiation, the spacing between the carbon shells increases from 3.4 to 3.8 Å due to the Na^+-ion insertion and the single-crystalline Co_9S_8 filler converts to numerous Co nanograins dispersed in a Na_2S matrix. Compared with the gentle microstructure evolution of the CNT under small charging voltage, a strong electrochemical reaction accompanying drastic swelling and fracturing of CNT shells is observed for the CNT electrode under large charging voltage. Our observations provide direct evidence and important insights for the electrochemical process of CNT-based composite materials in Na-ion batteries.

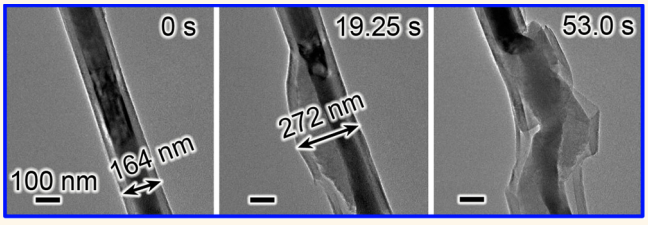

KEYWORDS: sodium-ion battery · carbon nanotube · *in situ* TEM · composite · sodiation

Advanced lithium-ion battery (LIB) technology has permeated portable electronics and has an important role in large-scale applications such as electric vehicles and stationary grid storage.[1,2] Extensive studies have been carried out to develop new high-capacity materials for higher-energy LIBs.[3,4] Substantial progress has been made in materials and chemistries to improve the battery technologies for transportation applications in electrical vehicles.[5−7] However, LIBs store electrical energy in electrodes through intercalation or insertion of lithium, which are prepared from limited Li-containing mineral resources. As the use of LIBs becomes widespread, increasing demand for Li commodity chemicals combined with geographically constrained Li mineral reserves will drive up the prices of LIBs. On the contrary, sodium (Na) is abundant (the fourth most abundant element in the earth's crust) and has a low redox potential[8] and is thus a favorable material to fabricate anodes of batteries at low cost. Therefore, Na-ion batteries are considered to be an attractive alternative to LIBs for meeting large-scale grid energy storage needs.[9]

Na-ion batteries have recently received great attention as an attractive electrochemical power source for energy storage,[10−12] spurred by the rapid advance in rechargeable battery technology and fast increasing demand in the market. However, Na^+ ions have a larger ionic radius than Li^+ ions, which makes it more difficult for them to be reversibly inserted into and extracted from host materials and more difficult to identify suitable electrode materials for

* Address correspondence to gaohuidu@zjnu.edu.cn, wenzhi.li@fiu.edu.

Received for review January 12, 2014 and accepted March 10, 2014.

Published online March 10, 2014
10.1021/nn500194q

Na-ion batteries.[13] Guided by the similar chemical nature of Li, many mature electrode materials for LIBs have been investigated as replacements for Na-ion batteries, such as hard carbon,[14,15] group IV elements like Si, Ge, or Sn,[16−18] intermetallic materials,[19] and various metal oxides[20,21] for the negative electrode, and $NaCrO_2$,[22] Na_xCoO_2,[23] $NaMnO_2$,[24] and $NaVPO_4F$[13] for the positive electrode. In fact, among numerous electrode materials for LIBs, only a few are suitable host materials to accommodate Na ions and allow reversible insertion/deinsertion reactions because of the larger ionic radius of Na. Therefore, the development of suitable anode materials for Na-ion batteries remains a considerable challenge. In contrast to the rich literature on LIBs, the science of Na-ion batteries is much less understood in most material systems. Therefore, the study on the fundamental mechanism of electrochemical sodiation of anode materials is urgent for the understanding and design of high-performance electrode materials for Na-ion batteries.

Carbon nanotube (CNT)-encapsulated cobalt sulfide composite presents one of the promising anode materials to replace carbonous anodes for the next-generation LIBs. However, it is still not clear if the composite can be applied in Na-ion batteries. In particular, the severe volume expansion of cobalt sulfide and the interaction between CNT sheath and cobalt sulfide filler during an electrochemical reaction remain unclear. Recently, *in situ* transmission electron microscopy (TEM) shows powerful application in the study of the dynamical electrochemical process of anode materials for LIBs,[25−34] but the study of the Na-ion battery is still very meager. In this work, we constructed successfully a nanosized Na-ion battery using individual Co_9S_8-filled CNTs as working electrodes inside a TEM, which allowed a real-time visualization of the electrochemical reaction process of Co_9S_8-filled CNTs with Na^+ ions for the first time. An in-depth understanding of the electrochemical process of CNT-based composites in a Na-ion battery was achieved.

RESULTS AND DISCUSSION

Figure 1a presents a schematic illustration of the all-solid nanoscale Na-ion battery that enables the *in situ* electrochemical experiments of an individual Co_9S_8-filled CNT. The nanosized electrochemical cell consisted of a Co_9S_8-filled CNT working electrode, Na metal counter electrode, and a solid electrolyte of naturally grown sodium oxide and hydroxide (Na_2O + NaOH) on the Na metal. The TEM image of a typical Co_9S_8-filled CNT used in this study is displayed in Figure 1b. Obviously, the CNT shows different contrast in regions A and B, suggesting a heterogeneous filling encapsulated inside the CNT. Figure 1c shows the HRTEM image of region A, which is a single-crystalline phase with fringe spacing of 0.49 and 0.30 nm, corresponding to the (002) and (311) planes of Co_9S_8.

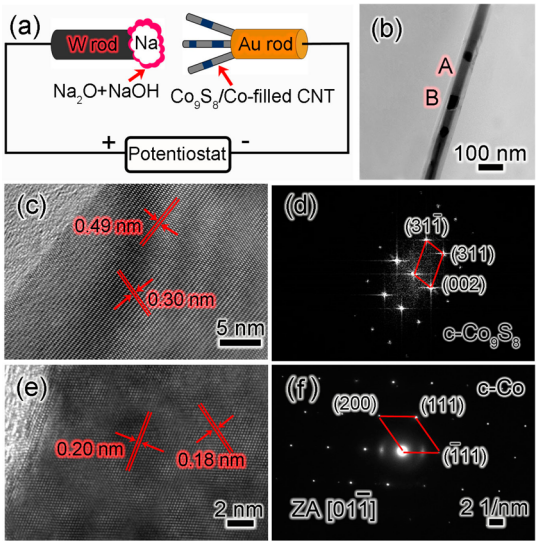

Figure 1. (a) Schematic illustration of the experimental setup for *in situ* TEM analysis of nanoscale Na-ion battery. (b) TEM image of a pristine Co_9S_8-filled CNT, consisting of two different regions, which are marked with letters A and B. (c) HRTEM image and (d) corresponding FFT pattern of region A. (e) HRTEM image and (f) EDP of region B.

The corresponding fast Fourier transform (FFT) pattern of the filler in the HRTEM image is given in Figure 1d and can be indexed as the cubic Co_9S_8 (a = 9.923 Å, JCPDF No. 86-2273). Figure 1e is a HRTEM image of region B; the filler is a single-crystalline phase, and the fringe spacing of 0.20 and 0.18 nm agrees with the (111) and (200) planes of cubic Co. The corresponding electron diffraction pattern (EDP) of region B is shown in Figure 1f, which can be well indexed to the (−111), (111), and (200) planes of cubic Co along the [01−1] zone axis (a = 3.545, JCPDF No. 15-0806). The TEM analysis of the sample reveals that the Co_9S_8 nanowires are largely encapsulated within the CNTs with the presence of a small amount of short Co segments. The elemental mapping of a filled CNT also suggests the existence of the Co segment in the CNT (Figure S1 in the Supporting Information). Since cobalt was used as catalyst for the filled CNT growth, nonreacted Co could remain and was encapsulated within the CNTs. In general, volume expansion, pulverization, and loss of electrical contact of electrode materials during the electrochemical reaction in the battery are the critical issues leading to rapid capacity decay. Although Co is inactive toward sodium, its presence is beneficial for the composite electrode by retaining a good conductivity.

The first sodiation process is critical for the electrode materials in Na-ion batteries because huge volume expansion takes place during this stage, which can lead to large irreversible capacity fading. To understand the microstructure evolution and electrochemical behavior of the Co_9S_8-filled CNT materials in Na-ion batteries, the electrochemical sodiation process of an individual Co_9S_8-filled CNT was investigated and is

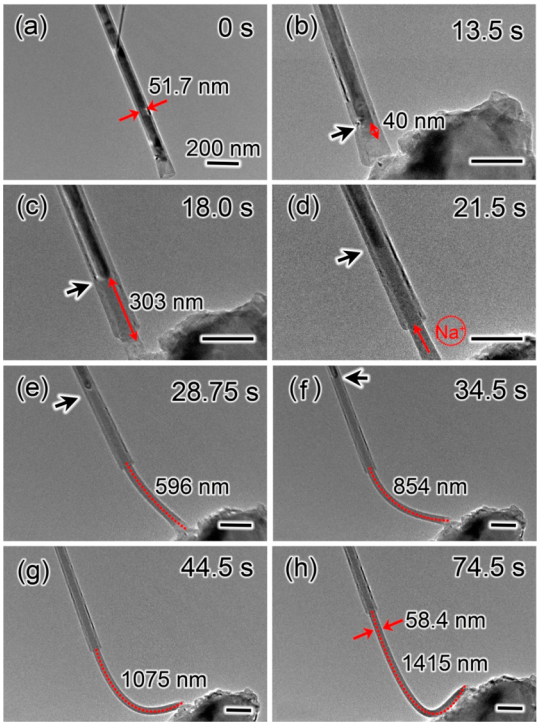

Figure 2. Time-resolved TEM images from video frames show the sodiation process of an individual Co_9S_8-filled CNT with an open end. (a) Individual Co_9S_8-filled CNT is selected as the working electrode; the diameter of the filling core is about 51.7 nm. (b−h) Time sequence of the sodiation process of the Co_9S_8-filled CNT, showing that the sodiated filler was squeezed out from the open end of the CNT. The sodiated Co_9S_8 nanowire expanded to 58.8 nm in diameter (h). A potential of −0.1 V was applied to the CNT electrode with respect to the Na metal. The red dotted lines demonstrate the extrusive part of the sodiated Co_9S_8. All scale bars are 200 nm.

shown in Figure 2 and movie S1 (in the Supporting Information). Figure 2a is the TEM image of a Co_9S_8-filled CNT with an open end, and the filler has a diameter of 51.7 nm before sodiation. After the front surface of the (Na_2O + NaOH) electrolyte touched the end of the Co_9S_8-filled CNT, the electrochemical sodiation process was initiated by applying a potential of −0.1 V on the CNT against the Na electrode to drive the flow of electrons and Na^+ ions across the circuit. Figure 2b−h shows the morphological evolution of this Co_9S_8-filled CNT electrode during the first sodiation. At 13.5 s (Figure 2b), a mild change could be observed in the Co_9S_8 encapsulated in the CNT compared with the image in Figure 2a. The sodiated phase showed a lighter contrast with a length of about 40 nm (the reaction front is marked by an arrow). After 18.0 s, the sodiated filler expanded its volume significantly and was extruded out of the CNT end; the reaction front was 303 nm from the open end of the CNT (Figure 2c), showing a migration speed of 58.4 nm/s. The filler was divided into two segments with different contrasts by the reaction front: one was the original Co_9S_8, and the other was the sodiated section. The length of the sodiated part continued to increase with the sodiation reaction. Figure 2d−h reveals the continuous elongation and extrusion of the sodiated Co_9S_8 filler, suggesting that the volume expansion is dominantly through axial elongation of the filler in open CNTs. Note that the reaction front, marked with black arrows in Figure 2, always kept a conical shape during the sodiation process, indicating that the Na^+ ions diffused through CNT shells faster than through the filler. In the beginning of the sodiation, the CNT was contacted with the electrolyte and Na^+ ions diffused mainly along the CNT wall. Subsequently, the CNT was shifted away from the electrolyte, and we found that the Na^+ ions could also diffuse easily through the sodiated Co_9S_8 nanowire. After a full sodiation process, the sodiated filler is 58.4 nm in diameter with a radial expansion of 12.9%; the sodiated nanowire extruded out of the open end of the CNT is 1415 nm in length with an axial expansion of about 120.8%. The volume expansion of the sodiated Co_9S_8 is found to be ∼181.7%, which is much larger than that of the Co_9S_8 (∼83.2%) as anode in LIBs owing to a large Na^+ ionic radius.[34] The migration speed of the reaction front through the sodiated filler part (Figure 2d−h) is lower than that through the CNT shells (Figure 2a−c), indicating the good conductivity of carbon for Na^+ ions. The results suggest that a small radial expansion occurs due to the mechanical constraint of the CNT while substantial axial elongation is inevitable for the filled CNT with an open end. The electrochemical sodiation process of another Co_9S_8-filled CNT with an open end was investigated, as shown in movie S2 in the Supporting Information. There was a small piece of carbon layer located at the interior of the CNT tip. Interestingly, the carbon layer was extruded out of the open end of the CNT by the outward-moving filler.

As mentioned above, the volume expansion, pulverization, and the loss of electrical contact of electrode materials are critical issues leading to rapid capacity decay in batteries. The intermittent Co segments in the Co_9S_8/Co-filled CNT composite are expected to improve the conductivity of sulfide and mediate the severe capacity decay. In our *in situ* TEM experiment, the Co segment was also monitored to investigate its response to the electrochemical process. Figure 3 and movie S3 in the Supporting Information show the details of the reaction front migration in a Co_9S_8/Co-filled CNT with an open end during the first sodiation process. The reaction front (marked by red dotted lines in Figure 3) propagated along the longitudinal direction of the CNT away from the solid electrolyte, and the Na^+ ions migrated as the electrochemical sodiation proceeded (Figure 3c). From Figure 3b,c, it can be clearly seen that the displacement of reaction front is ∼109 nm within 5.75 s, corresponding to a sodiation rate of ∼18.96 nm/s. The Na^+ ions can diffuse across the Co filler to continue the sodiation in the

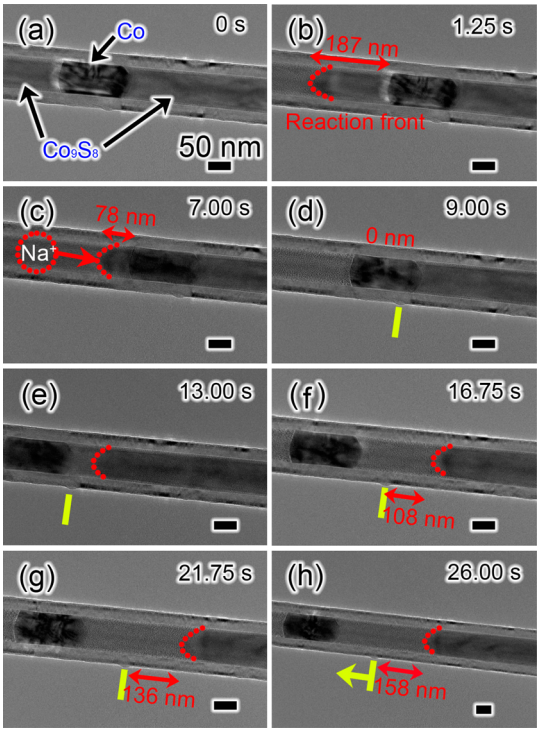

Figure 3. Time-resolved TEM images from video frames reveal the migration of the reaction front during the electrochemical sodiation process of a Co_9S_8/Co-filled CNT with an open end. (a–d) Sodiation of the first Co_9S_8 segment on the left of a Co block. (e–h) Sodiation of the second Co_9S_8 segment on the right of the Co block; the Co block was pushed backward due to the volume expansion of Co_9S_8. The reaction front was marked by the red dotted lines. A potential of −0.1 V was applied to the CNT electrode with respect to the Na metal. All scale bars are 50 nm.

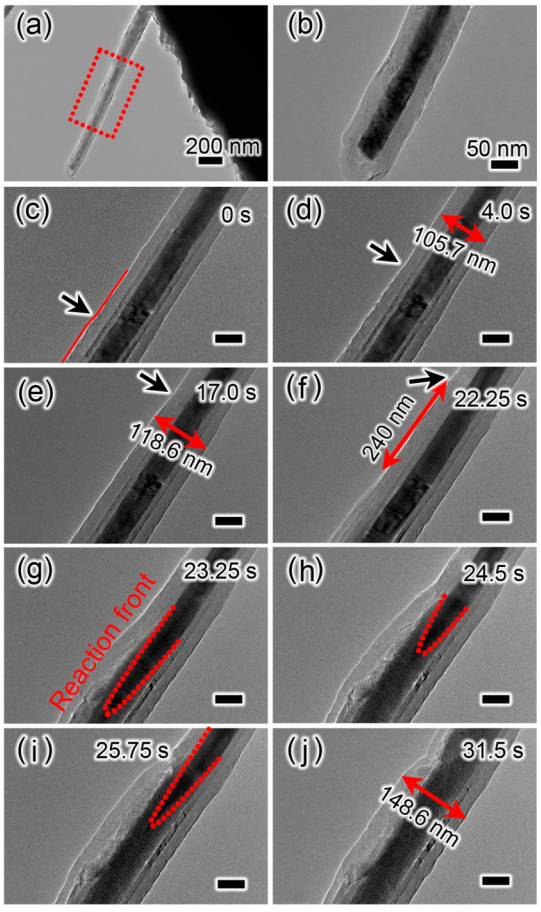

Figure 4. Time-resolved TEM images from video frames show the microstructural evolution of a part of a Co_9S_8-filled CNT with closed ends during sodiation with a potential of −0.1 V. (a,b) TEM images of the selected Co_9S_8-filled CNT with closed end. The sample is attached to the Au rod. (c) Video image of Co_9S_8-filled CNT recorded as the beginning (0 s), and the red line indicates the expansion of carbon shells. (d–j) Time sequence of the sodiation process of the Co_9S_8-filled CNT, showing a radial expansion of ∼12.2% during the Na^+ intercalation into the CNT and an extra radial expansion of ∼28.4% resulting from the sodiation of Co_9S_8 filler. The black arrows in (c–f) indicate the reaction front of the sodiation in the CNT wall. All scale bars are 50 nm.

second Co_9S_8 nanowire. It is noteworthy to mention that the Co block was pushed out toward the open end of the CNT owing to the expansion and extrusion of the second sodiated Co_9S_8 segment (denoted by yellow arrow and line in Figure 3d–h). The continuous sodiation of the second Co_9S_8 nanowire after the Co segment was revealed by the change of the texture of the Co_9S_8 filler in the TEM images (Figure 3d–h). At 16.75 s, the distance between the reaction front and the yellow marker is ∼108 nm, which increases to 158 nm at 26 s. It reveals that the reaction front of the second Co_9S_8 filler migrates about 50 nm within 9.25 s, corresponding to a sodiation rate of ∼5.4 nm/s, which is much slower than the sodiation of the first Co_9S_8 filler segment owing to the gradually increasing length of the diffusion path for Na^+ ions. In addition, the Co block was pushed backward about 168 nm within 17 s, corresponding to a moving speed of ∼9.88 nm/s. After the full electrochemical sodiation of the filled CNT with an open end, no visible crack and fracture was observed in the sodiated CNT, revealing a peaceful evolution.

There are two kinds of Co_9S_8-filled CNTs in the products in terms of the closed or open tips. Following the study on the sodiation behavior of a filled CNT with an open end, as shown in Figures 2 and 3, the sodiation of a Co_9S_8-filled CNT with a closed end was investigated and is shown in Figure 4 and movie S4 (in the Supporting Information). Figure 4a,b shows the TEM images of the selected Co_9S_8-filled CNT with a closed end. The sodiation process of a part of the filled CNT indicated by the dotted red box was monitored and is shown in Figure 4c–j. The Co_9S_8-filled CNT with the closed end exhibited significantly different sodiation behavior from the one with an open end. The state in Figure 4c was recorded as the beginning, in which the Co_9S_8 filler was fully encapsulated within carbon sheath so that it could not be extruded out during sodiation. The sodiation of carbon shells was first observed due to rapid diffusion of Na^+ ions on the CNT surface. The radial expansion of the sodiated CNT revealed the insertion of Na^+ ions into the carbon

shells. The reaction front (marked by the arrows) of carbon shells migrated along the CNT, and the filled CNT expanded from 105.7 to 118.6 nm in diameter after 4.0 s, corresponding to a radial expansion of about 12.2%. When Na^+ ions entered the tubes from either the surface defects or open ends, they diffused between the tube walls and interacted with neighboring carbon atoms. Figure 4c–e shows the sodiation of carbon shells, and the sodiation of the filler was not visible in the viewing area within 17.0 s. The larger radial expansion took place at 22.5 s (Figure 4f), suggesting the obvious sodiation of the Co_9S_8 nanowire, which lagged behind the sodiation reaction front of carbon shells by about 240 nm. Then a violent electrochemical reaction was exposed in Figure 4g. The strong volume expansion and structure change of the sodiated filler were observed. The reaction front marked with the red dashed line was a conical shape during the sodiation process. The volume expansion during the sodiation process was obvious in the radial direction. At 31.5 s, the filled CNT with the original diameter of 105.7 nm expanded to 148.6 nm, corresponding to a 40.6% radial expansion. This was in contrast to the sodiation of Co_9S_8-filled CNT with an open end, in which the radial expansion was weak while the axial expansion was considerable. The sodiated filler was not extruded out of the end of the CNT with the closed end because of the confinement of the carbon sheath. It was found that the electrochemical sodiation of the Co_9S_8-filled CNT with the closed end occurred in two steps, namely, the first rapid sodiation of CNT shells and the subsequent violent radial expansion of Co_9S_8 filler. The radial expansion of the CNT was about 12.2% due to the Na^+ intercalation into the graphite layers during the first step; an extra expansion of 28.4% was contributed by the swelling of the sodiated filler in the second step.

The rate performance is crucial for Na-ion battery electrodes. In general, the reversible capacity decreases for large charge/discharge current, which suggests different electrochemical behaviors at different current densities. The charge/discharge current can be adjusted by varying the sodiation voltage in the *in situ* TEM experiments. The electrochemical sodiation process of another Co_9S_8-filled CNT with closed ends under a larger bias is shown in Figure 5 and movie S5 (in the Supporting Information). The electrochemical sodiation process was initiated by applying a potential of −0.5 V to the Co_9S_8-filled CNT against the Na electrode, and the state in Figure 5a was recorded as the beginning of the sodiation process. Figure 5b–h shows the time-resolved TEM images from video frames during the first sodiation process. As shown in Figure 5b, the filled CNT expanded from 164 to 196 nm in diameter within 8.25 s. Continuous volume expansion of the sodiated filled CNT was observed in Figure 5c,d. The pristine filled CNT with the diameter

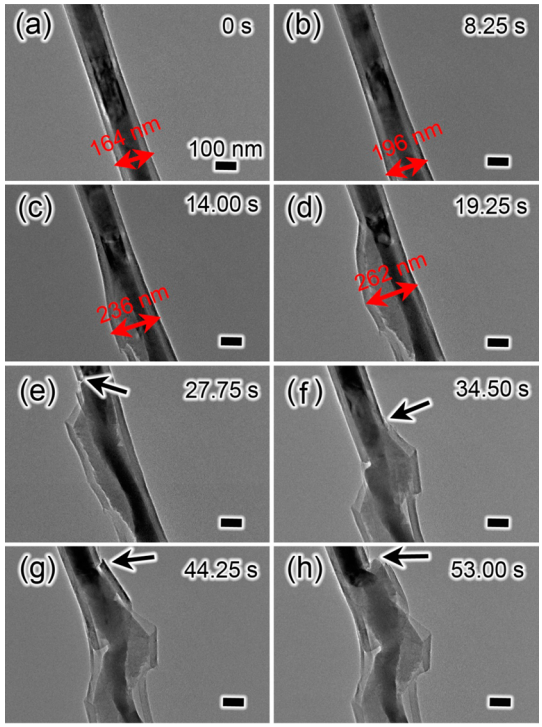

Figure 5. (a–h) Time-resolved TEM images from video frames reveal the appearance of fractures during the electrochemical sodiation process of an individual Co_9S_8-filled CNT with closed ends. The time sequence of the sodiation process shows the emergence and development of fractures and cracks in the Co_9S_8-filled CNT under a potential of −0.5 V. All scale bars are 100 nm.

of 164 nm was found to react quickly with Na^+ ions to form a sodiated product with a diameter of 262 nm within 19.25 s, corresponding to a local radial expansion of ~59.8% under the bias of −0.5 V. The Co_9S_8 filler expanded also from 100.2 to 183.8 nm in diameter. Then the intensive cracking and fracturing of the CNT sheath was observed. Figure 5e–h shows the appearance of a spate of fractures marked by the black arrows at different locations on the filled CNT. In the meantime, the volume expansion and pulverization of the Co_9S_8-filled CNT propagated quickly with the continuous sodiation. The explosive growth of many cracks and fractures of the sodiated CNT eventually leads to huge damage of the CNT sheath. As expected, the sodiation rate was much faster than the sodiation with the potential of −0.1 V, and the formation of crack and fracture was also found to be quite distinct from the sodiation at low potential. Our results suggest that a small current density is favorable for the electrode material in the first sodiation process by reducing the irreversible changes and weakening the formation of crack and fracture during the electrochemical reaction.

The electrochemical sodiation process of a single Co_9S_8/Co-filled CNT with closed ends under the potential of −0.5 V is displayed in Figure 6 and movie S6 in the Supporting Information. The dark segment was a Co particle; the Co_9S_8 nanowire filler was separated

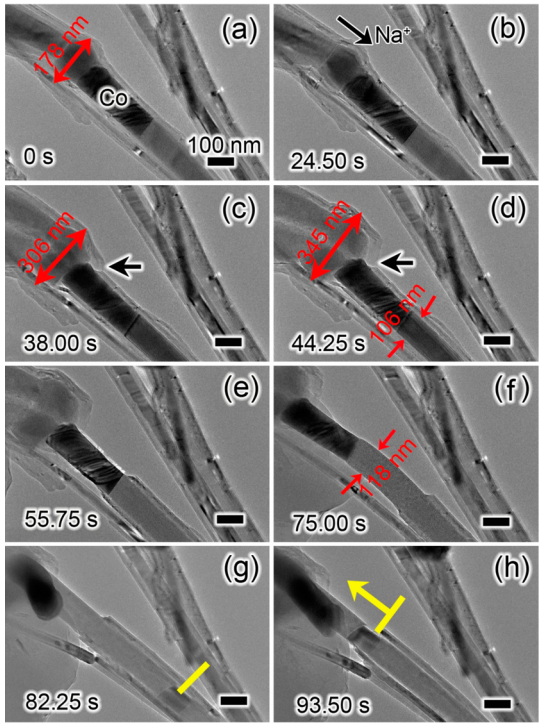

Figure 6. Time-resolved TEM images from video frames reveal the electrochemical sodiation process of a Co_9S_8/Co-filled CNT with closed ends under the potential of −0.5 V. (a−d) Electrochemical reaction of the upper side of the CNT filled with the first Co_9S_8 segment, showing the appearance of fracture and crack. The arrow in (b) indicates the sodiation direction. (e−h) Electrochemical reaction of the second Co_9S_8 segment, suggesting the sodiated Co_9S_8 and the Co block were squeezed out from CNT. The yellow bars indicate the position of the Co block, and the yellow arrow indicates the moving direction. All scale bars are 100 nm.

into two segments by this Co particle. Figure 6a−d shows the electrochemical sodiation reaction of the first Co_9S_8 segment. In contrast to the relatively peaceful sodiation process in the filled CNT with closed ends under a bias of −0.1 V, the electrochemical process under −0.5 V was quite violent, resulting in huge volume expansion and obvious fracture of the CNT (marked by the black arrow in Figure 6). After the sodiation for 44.25 s, the first CNT segment swelled dramatically from 178 to 345 nm in diameter, and the diameter of the Co_9S_8 filler expanded from 154 to 272 nm. The fracturing process of the CNT can be seen clearly in Figure 6c,d and movie S6. In the following electrochemical reaction process (Figure 6e−h), no further crack and fracture was observed since the cracked CNT would act like a CNT with an open end. So we can see that the Co particle and the sodiated Co_9S_8 nanowire were gradually squeezed out from the broken CNT due to the severe volume expansion of sodiated Co_9S_8. In the meantime, the rest of the CNT showed a small radial expansion; namely, the subsequent morphological changes were the same as that in the filled CNT with an open end shown in Figures 2 and 3. The Co filling part was completely extruded out

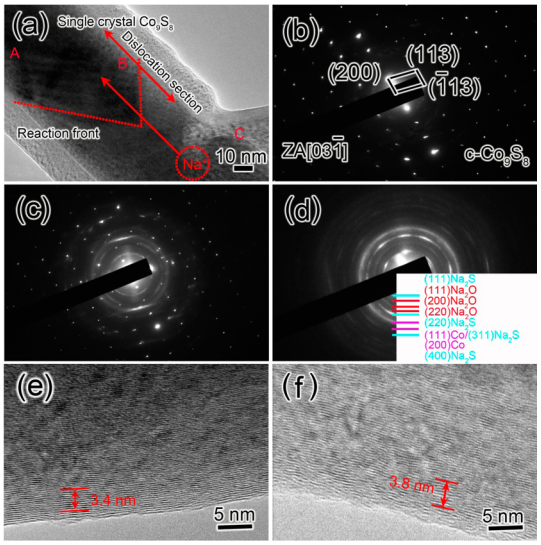

Figure 7. Structure and phase characterization of a Co_9S_8-filled CNT during the first sodiation process at −0.5 V against the Na metal electrode. (a) TEM micrograph of the filled CNT containing a reaction front separating the reacted and nonreacted sections. (b) SAED pattern of region A in image (a). (c) SAED pattern of reaction front (region B) in image (a). (d) SAED pattern of sodiated section (region C) in image (a). (e) HRTEM image of carbon shells of pristine CNT. (f) HRTEM image of carbon shells after sodiation.

of the carbon shells at 55.75 s. As the reaction front propagated, the length of the sodiated Co_9S_8 nanowire increased. The second Co_9S_8 nanowire with an initial diameter of 106 mm expanded to 118 nm (as shown by the arrows in Figure 6d,f), corresponding to a radial expansion of ∼11.3%. The sodiated Co_9S_8 nanowire began to bend rapidly at 75 s (Figure 6f) and formed a twisted nanowire (Figure 6h). It can be concluded that in the sodiation process under higher voltage the filled CNT with closed ends is prone to fracture due to the rapid volume expansion. The electrochemical lithiation of the Co_9S_8-filled CNT has been investigated using *in situ* TEM recently, and there was no obvious fracture observed in the CNT,[34] suggesting the electrode materials show different electrochemical behaviors in Na-ion batteries and LIBs.

Figure 7 shows a detailed structure and phase characterization of a Co_9S_8-filled CNT during the electrochemical sodiation process. A close inspection of the reaction front, shown in Figure 7a, revealed the presence of a region of a high density of dislocations separating the nonreacted and reacted regions of the filled CNT. Before reaction, the filler in the CNT was single-crystalline Co_9S_8 ($a = b = c = 9.923$ Å, JCPDF No. 86-2273) as confirmed by the selected area electron diffraction (SAED) (Figure 7b) recorded from region A marked in Figure 7a. Figure 7c displays the SAED pattern of the region around the reaction front (region B in Figure 7a), showing the coexistence of diffraction rings and spots. These diffraction spots were the same as that of the original Co_9S_8, and the

diffraction rings were from the resultant products by sodiation. This result suggests the coexistence of the pristine and sodiated Co_9S_8 in this region. A clear ring-like SAED pattern was obtained from a completely sodiated region (region C marked in Figure 7a) and is shown in Figure 7d. A few rings in the SAED pattern can be well indexed as Co and Na_2S phases, indicating that the Co_9S_8 phase was converted to Co and Na_2S during the electrochemical sodiation reaction. The rest of the diffraction rings fit the Na_2O phase. The formation of Na_2O may be attributed to the oxidation of the Na atoms by the absorbed oxygen on the CNT walls or the residue oxygen in the TEM column, which is similar to the formation of Li_2O on CNTs[35] and graphene nanoribbons[36] during electrochemical lithiation. From the HRTEM image of the carbon shell before (Figure 7e) and after (Figure 7f) electrochemical sodiation, the spacing of the (0002) plane of graphite was increased from 3.40 to 3.80 Å, confirming that Na^+ ions were indeed inserted into the intertubular gaps. The 11.8% interlayer expansion induced by sodium insertion on the CNT is quite larger than the lithiation-induced expansion (5.9%), which can be attributed to the larger ionic radius of sodium than that of lithium. The chemical composition of a Co_9S_8/Co-filled CNT before and after the sodiation was also investigated using energy-dispersive X-ray spectroscopy (EDX) (see Figure S1 in the Supporting Information). The elemental mapping of carbon, sulfur, and cobalt in the sodiated CNT is similar to that in the pristine CNT. The sodium and carbon elements exhibit the same distribution in the sodiated CNT, confirming that the Na^+ ions entered the CNT and reacted with the Co_9S_8. The elemental mapping results are consistent with the above HRTEM and SAED analysis.

CONCLUSION

In summary, the microstructural evolution and phase transformation of individual Co_9S_8-filled CNT during the first sodiation were revealed by constructing a nanoscale Na-ion battery using Co_9S_8-filled CNT as working electrode inside a TEM. Upon electrochemical sodiation of an open CNT, the sodiated Co_9S_8 filler is easily squeezed out of the CNT end due to the volume expansion while the CNT itself shows a small expansion in diameter. In contrast, the sodiated filler is still encapsulated within the CNT sheath due to the mechanical confinement of the carbon shells for a closed CNT that swells intensively due to the internal pressure resulted from the inflating Co_9S_8 filler. Therefore, the Co_9S_8-filled CNTs exhibit two kinds of behaviors during the first sodiation, namely, a notable axial elongation for an open CNT or a major radial expansion for a closed one. The spacing of the carbon shell increases from 3.4 to 3.8 Å owing to the Na^+ insertion. Compared with the peaceful microstructure evolution of the CNT under a bias of −0.1 V, violent electrochemical reaction and dramatic swelling and fracturing of the CNT wall were observed for the CNT electrode under a large bias of −0.5 V. The resulting sodiated Co_9S_8 consists of many Co nanograins embedded within a Na_2S matrix. Our studies shed light on the sodiation mechanism of nanostructure-filled CNT composites with potential application as anodes in high-performance Na-ion batteries.

EXPERIMENTAL SECTION

The Co_9S_8-filled CNT samples were synthesized using Co/MgO as catalyst by a thermal chemical vapor deposition (CVD) method.[37] The *in situ* nanoscale electrochemical experiments were conducted inside a JEM-2100F TEM with a Nanofactory TEM scanning tunneling microscopy (STM) holder. The accelerating voltage of the TEM was 200 kV with a point-to-point resolution around 0.18 nm. To prepare the nanosized Na-ion battery, Co_9S_8-filled CNTs were attached to a blunt Au wire (0.25 mm in diameter), serving as the working electrode. Bulk sodium metal was scratched with a sharp tungsten (W) tip, and the Na particles attached on W tip served as the counter electrode. A layer of Na_2O and NaOH mixture was grown on the Na particle surface due to the exposure to air during the loading process of the STM-TEM holder and served as the solid electrolyte for Na^+-ion transport. Both the CNT and Na electrodes were mounted onto a Nanofactory STM-TEM holder, which was quickly transferred into the TEM chamber with minimal exposure to air to enable the real-time observation of the electrochemical reaction and structural evolution of the Co_9S_8-filled CNT during the electrochemical sodiation process. During the experiments, the electron beam was blanked except for a short-time beam exposure for imaging to minimize the electron beam irradiation effect during the sodiation reaction.

Conflict of Interest: The authors declare no competing financial interest.

Acknowledgment. This work was supported by the Program for New Century Excellent Talents in University of Ministry of Education of China (NCET-11-1081), the National Science Foundation of China (No. 21203168), and the American Chemical Society Petroleum Research Fund under Grant No. 51766-ND10.

Supporting Information Available: Six videos showing the sodiation processes of individual Co_9S_8-filled CNTs. TEM images and elemental mapping of a Co_9S_8/Co-filled CNT before and after sodiation. This material is available free of charge *via* the Internet at http://pubs.acs.org.

REFERENCES AND NOTES

1. Dunn, B.; Kamath, H.; Tarascon, J. M. Electrical Energy Storage for the Grid: A Battery of Choices. *Science* **2011**, *334*, 928–935.
2. Yang, Z. G.; Zhang, J. L.; Kintner-Meyer, M. W. W.; Lu, X. C.; Choi, D.; Lemmon, J. P.; Liu, J. Electrochemical Energy Storage for Green Grid. *Chem. Rev.* **2011**, *111*, 3577–3613.
3. Armand, M.; Tarascon, J. M. Building Better Batteries. *Nature* **2008**, *451*, 652–657.
4. Aricò, A. S.; Bruce, P.; Scrosati, B.; Tarascon, J. M.; Schalkwijk, W. Nanostructured Materials for Advanced Energy Conversion and Storage Devices. *Nature* **2005**, *4*, 366–377.
5. Lou, X. W.; Archer, L. A.; Yang, Z. C. Hollow Micro-/Nanostructures: Synthesis and Applications. *Adv. Mater.* **2008**, *20*, 3987–4019.
6. Service, R. F. Getting There. *Science* **2011**, *332*, 1494–1496.
7. Kovalenko, L.; Zdyrko, B.; Magasinski, A.; Hertzberg, B.; Milicev, Z.; Burtovyy, R.; Luzinov, L.; Yushin, G. A Major

Constituent of Brown Algae for Use in High-Capacity Li-Ion Batteries. *Science* **2011**, *334*, 75–79.
8. Chevrier, V. L.; Ceder, G. Challenges for Na-Ion Negative Electrodes. *J. Electrochem. Soc.* **2011**, *158*, A1011–A1014.
9. Slater, M. D.; Kim, D.; Lee, E.; Johnson, C. S. Sodium-Ion Batteries. *Adv. Funct. Mater.* **2013**, *23*, 947–958.
10. Ponrouch, A.; Marchante, E.; Courty, M.; Tarascon, J. M.; Palacin, M. R. In Search of an Optimized Electrolyte for Na-Ion Batteries. *Energy Environ. Sci.* **2012**, *5*, 8572–8583.
11. Goodenough, J. B. Rechargeable Batteries: Challenges Old and New. *J. Solid State Electrochem.* **2012**, *16*, 2019–2029.
12. Barpanda, P.; Nishimura, S. I.; Yamada, A. High-Voltage Pyrophosphate Cathodes. *Adv. Energy Mater.* **2012**, *2*, 841–859.
13. Barker, J.; Saidi, M. Y.; Swoyer, J. L. A Sodium-Ion Cell Based on the Fluorophosphate Compound $NaVPO_4F$. *Electrochem. Solid-State Lett.* **2003**, *6*, A1–A4.
14. Xia, X.; Dahn, J. R. Study of the Reactivity of Na/Hard Carbon with Different Solvents and Electrolytes. *J. Electrochem. Soc.* **2012**, *159*, A515–A519.
15. Cao, Y. L.; Xiao, L. F.; Sushko, M. L.; Wang, W.; Schwenzer, B.; Xiao, J.; Nie, Z. M.; Saraf, L. V.; Yang, Z. G.; Liu, J. Sodium Ion Insertion in Hollow Carbon Nanowires for Battery Applications. *Nano Lett.* **2012**, *12*, 3783–3787.
16. Mortazavi, M.; Deng, J. K.; Shenoy, V. B.; Medhekar, N. V. Elastic Softening of Alloy Negative Electrodes for Na-Ion Batteries. *J. Power Sources* **2013**, *225*, 207–214.
17. Qian, J.; Chen, Y.; Wu, L.; Cao, Y.; Ai, X.; Yang, H. High Capacity Na-Storage and Superior Cyclability of Nanocomposite Sb/C Anode for Na-Ion Batteries. *Chem. Commun.* **2012**, *48*, 7070–7072.
18. Xu, Y. H.; Zhu, Y. J.; Liu, Y. H.; Wang, C. S. Electrochemical Performance of Porous Carbon/Tin Composite Anodes for Sodium-Ion and Lithium-Ion Batteries. *Adv. Energy Mater.* **2013**, *3*, 128–133.
19. Xiao, L. F.; Cao, Y. L.; Xiao, J.; Wang, W.; Kovarik, L.; Nie, Z. M.; Liu, J. High Capacity, Reversible Alloying Reactions in SnSb/C Nanocomposites for Na-Ion Battery Applications. *Chem. Commun.* **2012**, *48*, 3321–3323.
20. Su, D. W.; Ahn, H. J.; Wang, G. X. SnO_2@Graphene Nanocomposites as Anode Materials for Na-Ion Batteries with Superior Electrochemical Performance. *Chem. Commun.* **2013**, *49*, 3131–3133.
21. Xiong, H.; Slater, M. D.; Balasubramanian, M.; Johnson, C. S.; Rajh, T. Amorphous TiO_2 Nanotube Anode for Rechargeable Sodium-Ion Batteries. *J. Phys. Chem. Lett.* **2011**, *2*, 2560–2565.
22. Komaba, S.; Nakayama, T.; Ogata, A.; Shimizu, T.; Takei, C.; Takada, S.; Hokura, A.; Nakai, I. Electrochemically Reversible Sodium Intercalation of Layered $NaNi_{0.5}Mn_{0.5}O_2$ and $NaCrO_2$. *ECS Trans.* **2009**, *16*, 43–55.
23. Xia, X.; Dahn, J. R. A Study of the Reactivity of De-intercalated P_2-Na_xCoO_2 with Non-aqueous Solvent and Electrolyte by Accelerating Rate Calorimetry. *J. Electrochem. Soc.* **2012**, *159*, A647–A650.
24. Ma, X. H.; Chen, H. L.; Ceder, G. Electrochemical Properties of Monoclinic $NaMnO_2$. *J. Electrochem. Soc.* **2011**, *158*, A1307–A1312.
25. Su, Q. M.; Chang, L.; Zhang, J.; Du, G. H.; Xu, B. S. *In Situ* TEM Observation of the Electrochemical Process of Individual CeO_2/Graphene Anode for Lithium Ion Battery. *J. Phys. Chem. C* **2013**, *117*, 4292–4298.
26. Wang, C. M.; Xu, W.; Liu, J.; Zhang, J. G.; Saraf, L. V.; Arey, B. W.; Choi, D.; Yang, Z. G.; Xiao, J.; Thevuthasan, S.; *et al. In Situ* Transmission Electron Microscopy Observation of Microstructure and Phase Evolution in a SnO_2 Nanowire during Lithium Intercalation. *Nano Lett.* **2011**, *11*, 1874–1880.
27. Ghassemi, H.; Au, M.; Chen, N.; Heiden, P. A.; Yassar, R. S. *In Situ* Electrochemical Lithiation/Delithiation Observation of Individual Amorphous Si Nanorods. *ACS Nano* **2011**, *5*, 7805–7811.
28. Gu, M.; Li, Y.; Li, X. L.; Hu, S. Y.; Zhang, X. W.; Xu, W.; Thevuthasan, S.; Baer, D. R.; Zhang, J. G.; Liu, J.; *et al. In Situ* TEM Study of Lithiation Behavior of Silicon Nanoparticles Attached to and Embedded in a Carbon Matrix. *ACS Nano* **2012**, *6*, 8439–8447.
29. Su, Q. M.; Dong, Z. M.; Zhang, J.; Du, G. H.; Xu, B. S. Visualizing the Electrochemical Reaction 0f ZnO Nanoparticles with Lithium by *In Situ* TEM: Two Reaction Modes Are Revealed. *Nanotechnology* **2013**, *24*, 255705.
30. Wang, J. W.; Liu, X. H.; Zhao, K. J.; Palmer, A.; Patten, E.; Burton, D.; Mao, S. X.; Suo, Z. G.; Huang, J. Y. Sandwich-Lithiation and Longitudinal Crack in Amorphous Silicon Coated on Carbon Nanofibers. *ACS Nano* **2012**, *6*, 9158–9167.
31. Zhang, L. Q.; Liu, X. H.; Liu, Y.; Huang, S.; Zhu, T.; Gui, L. J.; Mao, S. X.; Ye, Z. Z.; Wang, C. M.; Sullivan, J. P.; *et al.* Controlling the Lithiation-Induced Strain and Charging Rate in Nanowire Electrodes by Coating. *ACS Nano* **2011**, *5*, 4800–4809.
32. Huang, J. Y.; Zhong, L.; Wang, C. M.; Sullivan, J. P.; Xu, W.; Zhang, L. Q.; Mao, S. X.; Hudak, N. S.; Liu, X. H.; Subramanian, A.; *et al. In Situ* Observation of the Electrochemical Lithiation of a Single SnO_2 Nanowire Electrode. *Science* **2010**, *330*, 1515–1519.
33. Liu, X. H.; Liu, Y.; Kushima, A.; Zhang, S. L.; Zhu, T.; Li, J.; Huang, J. Y. *In Situ* TEM Experiments of Electrochemical Lithiation and Delithiation of Individual Nanostructures. *Adv. Energy Mater.* **2012**, *2*, 722–741.
34. Su, Q. M.; Du, G. H.; Zhang, J.; Zhong, Y. J.; Xu, B. S.; Yang, Y. H.; Neupane, S.; Kadel, K.; Li, W. Z. *In Situ* Transmission Electron Microscopy Investigation of the Electrochemical Lithiation−Delithiation of Individual Co_9S_8/Co-Filled Carbon Nanotubes. *ACS Nano* **2013**, *7*, 11379–11387.
35. Liu, Y.; Zheng, H.; Liu, X. H.; Huang, S.; Zhu, T.; Wang, J. W.; Kushima, A.; Hudak, N. S.; Huang, X.; Zhang, S. L. Lithiation-Induced Embrittlement of Multiwalled Carbon Nanotubes. *ACS Nano* **2011**, *5*, 7245–7253.
36. Liu, X. H.; Wang, J. W.; Liu, Y.; Zheng, H.; Kushima, A.; Huang, S.; Zhu, T.; Mao, S. X.; Li, J.; Zhang, S. L.; *et al. In Situ* Transmission Electron Microscopy of Electrochemical Lithiation, Delithiation and Deformation of Individual Graphene Nanoribbons. *Carbon* **2012**, *50*, 3836–3844.
37. Du, G. H.; Li, W. Z.; Liu, Y. Q. Filling Carbon Nanotubes with Co_9S_8 Nanowires through *In Situ* Catalyst Transition and Extrusion. *J. Phys. Chem. C* **2008**, *112*, 1890–1895.